Mammalian-like developmental changes are present in the neural signatures of avian sleep

Hamed Yeganegi[1,2] and Janie M. Ondracek[1]*

[1]Chair of Zoology, Technical University of Munich, Liesel-Beckmann-Str. 4, 85354 Freising-Weihenstephan, Germany

[2]Graduate School of Systemic Neurosciences, Ludwig-Maximilians-University Munich, Großhaderner Str. 2, 82152 Planegg, Germany

[*] Corresponding author

Summary

Despite their phylogenetic differences and distinct pallial structures, mammals and birds share many features of sleep structure, most prominently, the existence of distinct stages of rapid eye movement (REM) and slow wave sleep (SWS).[1-4] However, the structure of sleep does not remain constant during lifetime, but undergoes radical changes during development.[5] Our current understanding of these age-related variations in neural signature of sleep is limited to studies in a small number of mammalian species.[5-7] How does the neural signature of sleep evolve during brain development in an avian brain? To answer this, we recorded multi-channel EEG from developing juvenile and adult zebra finches for several nights. We compared the structure of sleep in adults and juveniles using the ratio of slow oscillations to gamma oscillations ("depth of sleep", DOS). We observed a significantly larger DOS, as well as less-frequent state transitions in juveniles compared to adults. Furthermore, multichannel EEG revealed local slow oscillations, in addition to global (wide-spread) slow waves. The occurrence of these local waves was correlated with DOS and was higher in frontal sites. In addition, we observed that the functional connectivity increased rapidly during development and was significantly higher in adults than in juveniles. Complementarily, a graph theory analysis of highly-correlated networks revealed numerous small networks in juveniles compared to adults, underscoring the lower connectivity observed in juveniles. Overall, our results reveal significant changes in the neural signature of sleep during development in an avian brain that are remarkably similar to age-dependent changes that occur in mammals.

Keywords: sleep, avian sleep, EEG, functional connectivity, zebra finch, brain development, slow waves

Introduction

Sleep is a reversible state characterized by a reduced level of behavioral activity and responsiveness to the environment, and which typically adheres to a circadian rhythm. It has been observed across animal taxa including early animals without a centralized nervous system, such as the cnidarian.[8,9]

However, sleep is not a homogeneous state.[10] The current definitions of sleep in mammals and birds, categorized sleep time into “REM” or “rapid-eye-moment”, and non-REM sleep stages.[11,12-14] As a human falls asleep, the dominance of high-frequency, low-amplitude oscillations of the awake electroencephalography (EEG) is replaced by slower, higher amplitude oscillations that indicate the onset of a non-REM sleep stage.[14] A non-REM period usually culminates in slow wave sleep (SWS), when large slow oscillations (frequency < 1 Hz) dominate the EEG. After a non-REM stage, the EEG starts to show abundant theta and gamma activity, which concurs with skeletal-muscle atonia and the characteristic rapid eye movements, marking the onset of a rapid eye movement sleep (REM) period.[14,12] These periods of non-REM and REM occur alternatively several times during the sleep period.[14] It is worth mentioning that in birds, the non-REM sleep could be subdivided into SWS and intermediate stage (IS), the latter being reminiscent of early stages of mammalian non-REM that occurs before a SWS stage.[1,2]

Recent studies have shown the existence of similar two-stage structure of sleep with distinct neural correlates in a wider range of species including two species of lizards and a teleost fish.[15-17] Furthermore, newly emerging evidence from the cuttlefish and fruit fly extends the understanding of multiple stages of sleep beyond vertebrates.[18-20]

Comparably, birds share several similarities with mammals regarding the organization of sleep into REM and non-REM stages.[1,2,21] However, the limited number of studies in avian species have focused primarily on adult birds,[1-3,22-24] and the previous studies on immature birds [25-27] do not provide a comprehensive picture of the neurobiology of avian sleep as a function of development and aging.

Many species of birds, including the zebra finch, undergo vocal learning, which is a developmentally restricted ability to learn new vocalizations based on auditory feedback and motor learning experienced as a juvenile. Considering the extensive alterations in sleep architecture that occur during development and across aging,[28] as well as the paucity of information available about sleep in juvenile birds, it is of major interest to characterize sleep features across different ages of birds to examine whether there are clear differences between sleep features in adult and juvenile zebra finches.

Results

Sleeping brain dynamics are larger and more variable in juveniles compared to adults

In order to investigate the role of sleep oscillations during brain development, we chronically implanted 10 zebra finches (3 adults; 7 juveniles; for ages see Table 1 in Methods) with custom-designed electrodes to record supra-dural electroencephalogram (EEG) from 16 sites over a wide surface area of the skull (approx. 7 mm × 8 mm; Figure 1A). We recorded brain activity during 12-hour periods of natural sleep for 49 total nights across animals (more than 600 hours

of data for all animals). During sleep, animals assumed typical postures of sleep in birds, with the head bent forward or sidewise and tucked under the wing. The body movement, as assessed with video recordings throughout the night, was generally low (Figure 1B, Figure S1A).

For each night, we compared the structure of sleep in adults and juveniles by calculating the ratio of slow oscillations to gamma oscillations ("depth of sleep", DOS). This metric is analogous to those used in mammals,[29,30] but accounts for the frequency bands prevalent in avian EEG,[1] (see discussion for explanation of the use of this continuous measure of brain state instead of discrete sleep staging). We calculated the DOS as the ratio of the relative power of the delta and theta bands (1.5-8 Hz) to the gamma band (30-49 Hz)

We observed that across animals, the DOS generally varied on the order of tens of seconds (Figure 1B, Figure S1A). We examined the raw EEGs at high, middle and low points of the DOS, and found that high DOS corresponded to EEGs typical of slow wave sleep (SWS), and that low DOS corresponds to typical of rapid eye movement (REM) sleep (Figure 1C; Figure S1B), verifying the use of DOS as a method to estimate sleep stages. Middle DOS values correspond to intermediate stage (IS) of sleep and are comparable to stage 1 and 2 of non-REM sleep in human.[2] Although we used a single channel to calculate the DOS across animals (channel 4 in Figure 1A; black arrow in Figure 1C), the global aspects of sleep were comparable when other channels were used for both adults and juveniles (Figure 1D). Indeed, the DOS correlation was high when calculated across all channels and averaged across all birds for one night of sleep (correlation coefficient = 0.59 ± 0.14; mean ± SD)

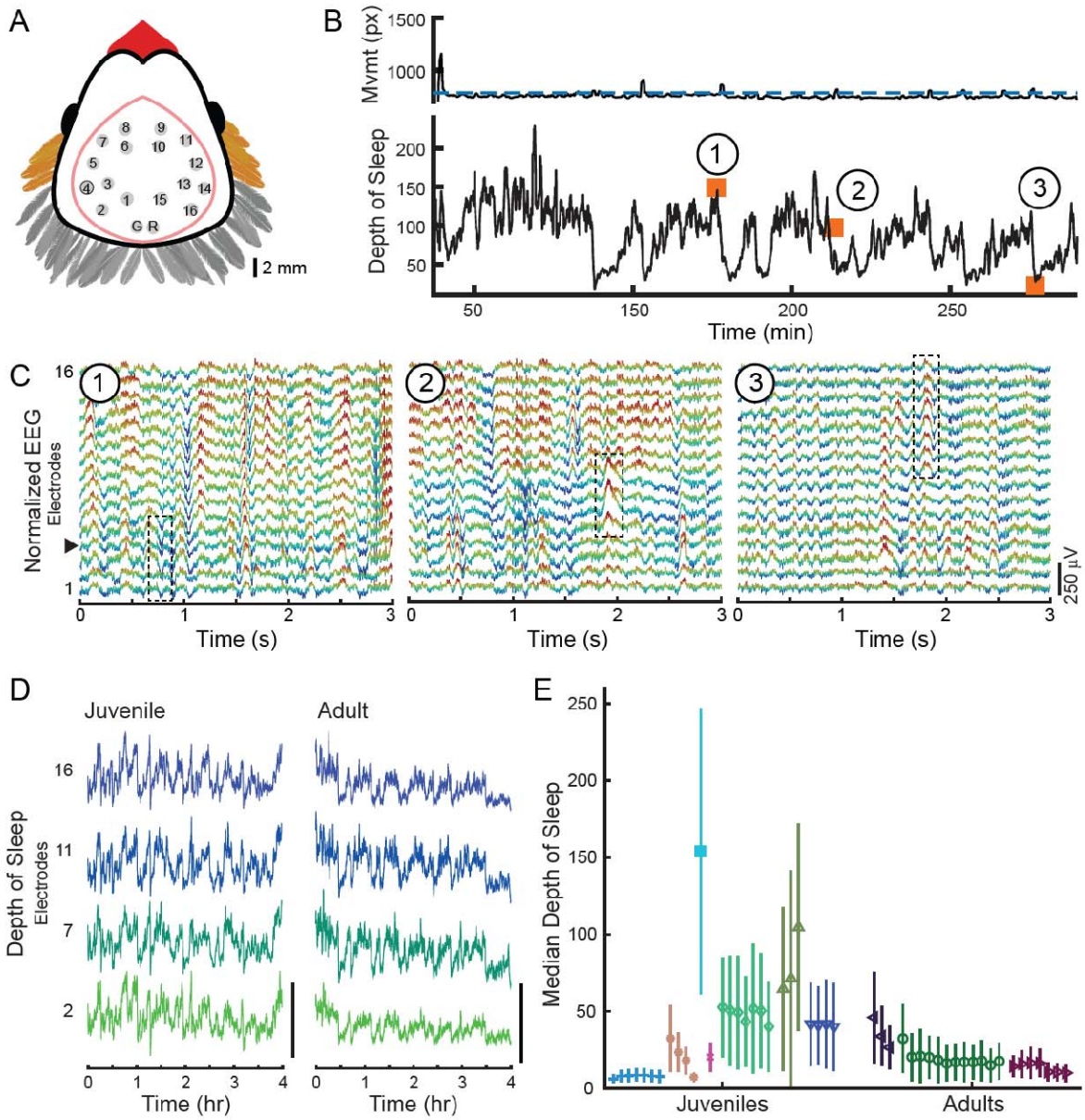

Figure 1. Multichannel EEG recording during sleep and corresponding DOS. (A) EEG electrode sites: 8 electrode sites on each hemisphere covered wide area over the surface of pallium. (B) Top: Movement extracted from the infrared video recording (px, pixels). Blue line is the threshold delineating wake/sleep. Bottom: Corresponding DOS ratio shows the fluctuations in the oscillatory components of EEG. Movement and DOS smoothed with a 30-secs window for visualization purposes. Orange squares 1, 2, and 3, correspond to EEG data in C. (C) 3-s examples of EEG from SWS, IS, and REM sleep, respectively. Color scheme is for visualization purposes only. This amplitude-coding color scheme helps visually identifying waves that occur simultaneously across several channels. Black dotted box highlights local waves. (D) In the time scale of minutes, the general oscillatory mode of brain, represented by DOS, is similar across channels. Error bar is 200 (unit-less DOS ratio). (E) DOS across all the nights for each bird (median ± interquartile interval computed over all the 3-sec bins over the night). DOS is relatively consistent across nights in each individual bird, but a large inter-subject variability was observed.

We calculated the median DOS value for each 12-hour night of sleep for each animal and found that although the median variability varied widely across animals, it was largely the same for different nights of sleep within the same animal (Figure 1E). This finding mirrors results from studies of human sleep, where distinct inter-individual differences in EEG have also been observed in humans.[31]

When comparing median DOS of each night, between adults and juveniles, we found that the median DOS pooled across all juvenile nights of sleep (n = 27 nights) was significantly larger compared to the adult nights of sleep (n = 22 nights of sleep; DOS = 49.9 ± 32.2 (mean ± SD) in juveniles versus 19.5 ± 8.4 in adults; Wilcoxon rank-sum test, $p = 1.6\times10^{-5}$). To see whether this difference in DOS is due to the difference in the low frequencies or the gamma frequency, we also compared the power in each of these bands across juvenile and adult groups (Supplementary Figure 2A). It showed that the relative power of gamma band was not different across the groups (0.0040 ± 0.0050 in juveniles and 0.0038 ± 0.0052 in adults, mean ± SD, scale-free due to relative power, p = 0.55, Wilcoxon rank-sum test). However, indeed the relative power in the low-frequencies, was significantly higher in the juveniles than in adults (0.88 ± 0.059 in juveniles and 0.062 ± 0.080 in adults, p = 0.02, Wilcoxon rank-sum test). This suggests that the Delta and Theta oscillatory components of EEG, i.e. 1.5 - 8 Hz waves, decrease after maturation.

Juveniles transition through sleep states less frequently than adults

In order to get a sense of the frequency of state transitions in juveniles versus adults (Figure 2A), we detected the peaks and troughs of the unsmoothed DOS and calculated the transitions from SWS (high DOS) to REM (low DOS) for all juvenile and adult nights of sleep (Methods). The transition frequency was relatively constant when pooled over adults (approximately 45 transitions per hour throughout the night; Figure 2B). In juveniles however, the transition frequency varied throughout the night and ranged from approximately 45 transitions per hour at the beginning of the night to approximately 30 transitions per hour in the middle of the night (Figure 2B), before increasing to over 50 transitions during the last hours of sleep. This difference between adults and juvenile was significant for the 4th, 5th, and 6th hours of sleep, (Wilcoxon rank-sum test, p-values = 0.045, 0.001, and 0.0005 respectively).

The average inter-SWS interval was significantly longer in juveniles compared to adults (92.86 ± 121.41 sec versus 82.84 ± 102.80 sec, unpaired t-test, $p = 5.7\times10^{-12}$). Similarly, the average inter-REM interval was also significantly longer in the juveniles compared the adults (92.88 ± 115.07 versus 82.74 ± 99.15, unpaired t-test, $p = 5.5\times10^{-13}$). It should be noted that we have only considered the SWS-to-SWS periods that enclosed a REM occurrence in between, i.e., SWS-REM-SWS, and not SWS-IS-SWS. The same is true for inter-REM transitions: we only considered REM-SWS-REM transitions, and not REM-IS-REM.

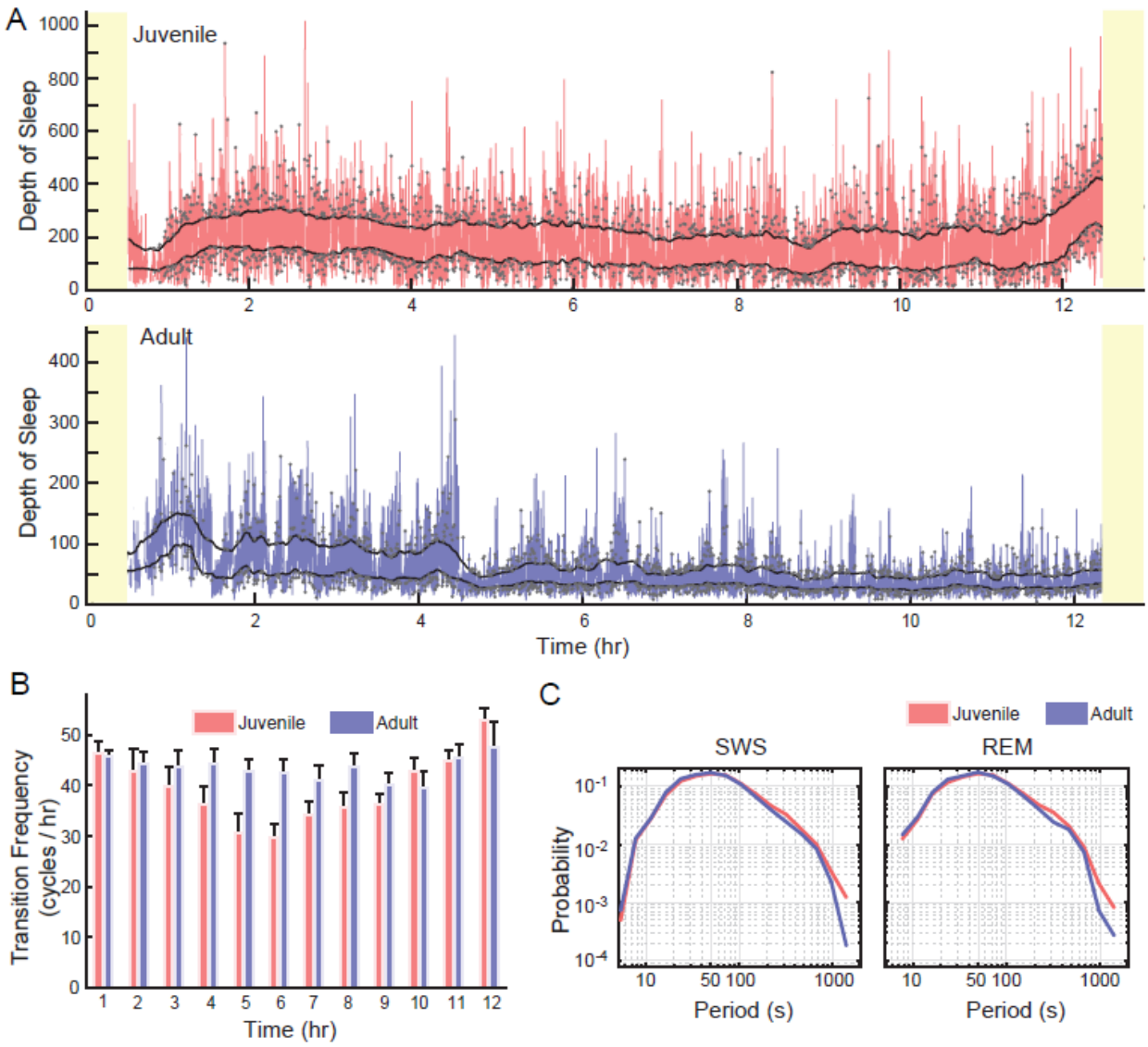

Figure 2. State transitions during sleep. (A) The unsmoothed DOS (red, juvenile; blue, adult; same animals as depicted in Fig. 1) is plotted for the whole night of sleep. State-transitions are indicated as small gray dots. In each DOS plot, the upper and lower black lines demarcate the SWS and REM detection thresholds. Gray dots indicated the bin when there has been a threshold-crossing from REM to SWS (upper dots) or SWS to REM (lower dots). The yellow bars indicated periods of lights on. (B) Bar plot indicates the number of SWS-to-REM transitions per hour during night in juveniles and adults. The frequency of state transitions remains relatively constant during the night in the adults. In contrast, the state transitions for juveniles are not constant: interestingly, during the middle of the night (i.e., the 5th, 6th, and 7th hours), the state-transition frequency is significantly lower in juveniles than for adults, suggesting that the juvenile brain spends longer periods of time in REM or SWS sleep. The state transition frequency increases again at the end of the night of sleep in juveniles. (C) The probability distribution function of inter-SWS and inter-REM intervals. In both cases the probability of observing longer periods of SWS or REM is significantly higher in the juvenile group; Inter-SWS interval was 92.86 ± 121.41 sec in juveniles and 82.84 ± 102.80 sec in adults (unpaired t-test, p = 5.7×10-12). Similarly, inter-REM interval was

significantly longer in the juveniles (92.88±115.07 in juvenile similar to observations in human EEG, and 82.74±99.15 in adults, unpaired t-test, p = 5.5×10-13).

Local waves are more frequent in adults compared to juveniles

Although we observed that the global characteristics of sleep were highly similar across recording sites (Figure 1D), we nevertheless observed short duration (10-100 ms) local differences, or “local waves” that spread across a limited number of the EEG electrodes (similar to observations in human EEG,[32] Fig. 1C; black boxes). Here we defined them as waves that are observable at least in 25% of channels, but not more than 75% of them (see methods for the detail of wave detection). It should be noted that these local waves are distinct from unihemispheric SWS activity,[33] in which patterns of SWS (on the order of tens of second or longer) are observed across one whole hemisphere but not the other.

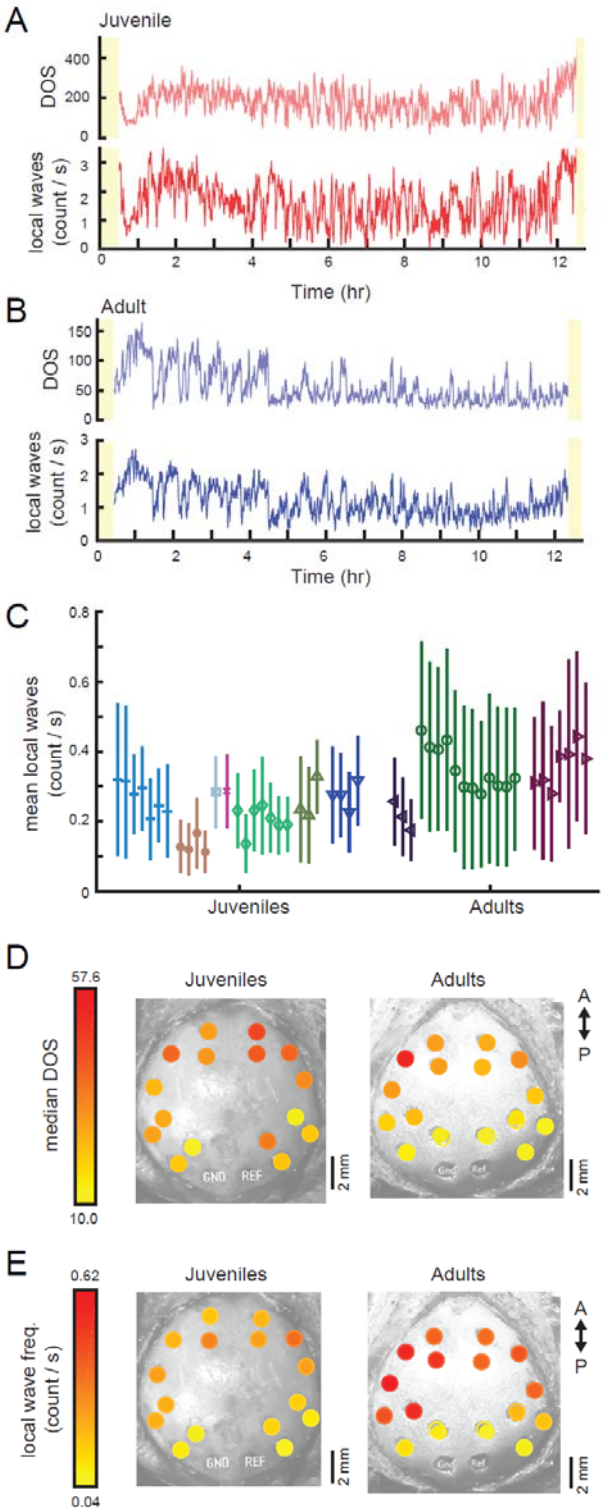

Figure 3. Local waves frequency is different across age groups and has a posterior-anterior axis. (A) Juvenile DOS (top, light red line) and the corresponding rate of occurrence for local waves (bottom, dark red line) for a whole night of sleep (same juvenile as in Fig. 1). The occurrence of local waves is

correlated with the DOS, i.e., it is high during high DOS values (i.e., high power in low frequencies), and is low for low DOS values (i.e., low power in low-frequencies). The data have been smoothed with a moving average filter with a window of length equal to 10 for visualization purposes. (B) Adult DOS (top, light blue line) and the corresponding rate of occurrence for local waves (bottom, dark blue line) for a whole night of sleep (same adult as in Fig. 1). Figure conventions same as in (A). (C) The average rate of occurrence for local waves across nights for all birds. Each color indicates a different bird, and the vertical line indicates the SD for the night. Local waves occur significantly more frequently in the adult birds compared to juveniles ($p = 7.0\times10^{-9}$, Wilcoxon rank-sum test). The data for each bird was sorted based on the day of recording, not the actual age. (D) Average DOS computed at each electrode site across all juveniles (left) and all adults (right). DOS is higher in anterior regions (red colors) as compared to posterior sites (yellow colors). This anterior-posterior gradient is especially pronounced in the adult brain. (E) Average rate of local waves computed at each electrode site across all juveniles (left) and all adults (right). Same figure conventions as for (D). An anterior-posterior gradient is also observable here, such that anterior regions have a higher rate of local wave occurrence (red colors) compared to posterior sites (yellow colors).

We quantified the occurrence of local waves in relation to the DOS in juveniles and adults (Figure 3A, 3B). The occurrence of local wave was correlated with the DOS; that is, we observed that for periods of high DOS, there was a corresponding increase in the number of local waves. The correlation between the DOS and the occurrence of local waves, calculated across all nights in 3-s bins, was significant and relatively high for adults (0.52 ± 0.14; $p = 4.0\times10^{-5}$; $n = 22$ nights; median ± interquartile interval, Wilcoxon rank-sum test). The correlation between the DOS and the occurrence of local waves for juveniles, while lower, was also significant (0.30 ± 0.28; $p = 1.2\times10^{-5}$; $n = 27$ nights; Wilcoxon rank-sum test).

In terms of the actual occurrence of local waves, number of detected local waves per second was significantly higher for adults than for juveniles; 0.33 ± 0.21 versus 0.22 ± 0.12 (mean ± SD), $p = 7.0\times10^{-9}$, Wilcoxon rank-sum test (Figure 3C).

It is well known that during human sleep, anterior EEG sites display larger slow waves compared to posterior positions; that is, there is an anterior-posterior asymmetry in slow wave activity (SWA).[34,35,36] We were curious to see if slow waves and local waves were similarly localized to a certain parts of the avian brain. We observed that - similar to humans - anterior EEG sites, in both adults and juveniles, exhibit larger DOS values compared to posterior positions (Figure 3D; red colors). We observed a similar trend for the local waves: the median local waves were more numerous in anterior sites compared to posterior sites, especially for adults (Figure 3E; red colors). These findings suggest that there could be a developmental component to localization of local waves to anterior sites, such that during the process of brain maturation and cortical specialization, the neuroanatomical development of the avian brain facilitates the spread of low-frequency oscillations (1.5-8 Hz) in anterior sites.

Functional connectivity during development

It is generally accepted that in mammals, cortical EEG activity during REM sleep is desynchronized, whereas EEG activity during non-REM sleep becomes synchronized.[10] However, this understanding is complicated by evidence of highly-synchronized beta and gamma activity during REM,[37] and local (desynchronizing) activity during non-REM.[38] In order to

better understand the synchronous aspects of sleep in birds, we investigated EEG synchrony across and within hemispheres during sleep in adults and juveniles.

To quantitatively characterize the synchrony of neural activity at the hemispheric level, we used a common measure of functional connectivity,[39] the between-channel correlation coefficient (CC; Methods). We analyzed CCs for all pairs of intra-hemispheric (Figure 4A; L-L pairs and R-R pairs) and inter-hemispheric channels (Figure 4A, L-R pairs).

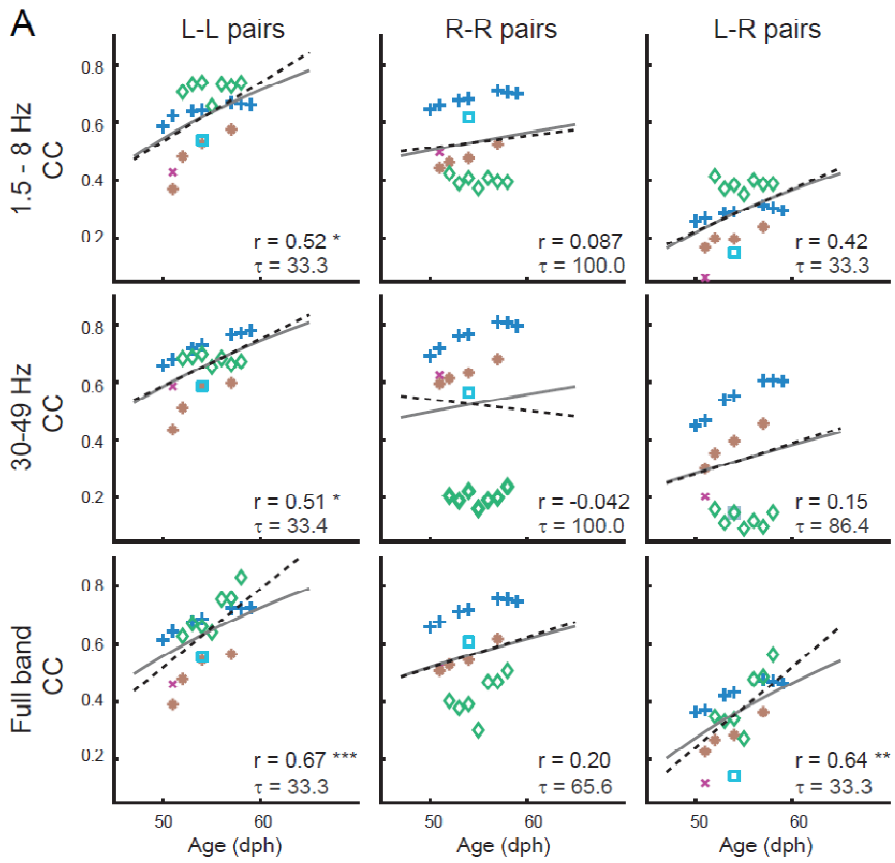

Figure 4. Functional connectivity increases during development in juveniles.

(A) The functional connectivity, defined here as the correlation coefficient (CC), was computed between pairs of channels from the left hemisphere (L-L; left column), right hemisphere (R-R, middle column), or opposite hemispheres (L-R; right column) as a function of juvenile age. Colors represent different juveniles, and each marker represents the mean CC across channels for a night of sleep. The connectivity was computed on EEG in the lower bands (1.5 - 8 Hz; top row), higher band (30 - 49 Hz; middle row), and the full-band (1.5 - 200 Hz; bottom row). The intra-hemispheric CC values (i.e., L-L and R-R pairs) were greater than the inter-hemispheric CC values (L-R pairs), suggesting there is larger connectivity within the same hemispheres in juveniles. An exponential fit of the data (gray line; see text for details) showed that although time constant (τ) differs across conditions, all cases yielded a time constant of approximately 30-90 days, implying a fast rate of increased connectivity during development. The steepness of the linear fit of the data plotted as a function of age (black line) was higher for L-L pairs compared to R-R pairs, suggesting that L-L connections might form more quickly in time than R-R connections. Asterisks indicate significant linear fits (*, $p \leq 0.05$; ** $p \leq 0.01$; ***, $p \leq 0.001$).

Intra-hemispheric connectivity is larger than the inter-hemispheric connectivity

We observed significant differences when connectivity was compared across L-L, R-R, and L-R pairs (2-way ANOVA, $p = 7.3\times10^{-8}$ in adults and $p = 3.3\times10^{-5}$ in juveniles). In adults, the average intra-hemispheric correlations were 0.62 ± 0.16 (L-L pairs; mean ± SD) and 0.57 ± 0.14 (R-R pairs). In contrast, the average inter-hemispheric correlation for L-R pairs was 0.27 ± 0.15, less than half of the intra-hemispheric correlations. The same pattern was true for the intra-hemispheric and the inter-hemispheric correlations in juveniles (L-L = 0.54 ± 0.15; R-R = 0.51 ± 0.11; L-R = 0.26 ± 0.16). The difference between inter-hemispheric connectivity (L-R) and the intra-hemispheric connectivities (L-L and R-R) was significant for both adult and juvenile group ($p = 9.1\times10^{-10}$ in adults and $p = 9.0\times10^{-10}$; post-ANOVA Tukey-Kramer multiple comparison test).

Moreover, we observed that in adult birds, but not the juveniles, the connectivity changes significantly across sleep stages (Friedman test, p=0.003 in adults, and p=0.66 in juveniles). The connectivity was highest during SWS, CC=0.52±0.29 (mean ± SD), and lowest during REM, CC=0.49 ± 0.27, when averaged over all pairs of channels in adult data (n=2299 pair of channels in total).

Hemispheric asymmetry observed in adult birds

Notably, in the adult group, the connectivity in the left hemisphere was significantly higher than the connectivity in the right hemisphere (L-L = 0.62 ± 0.16 versus R-R= 0.57 ± 0.14; p = 0.03, post-ANOVA Tukey-Kramer multiple comparison test). However, in the juveniles, the intra-hemispheric correlations were only slightly different (L-L = 0.54 versus R-R = 0.51), and this difference was not significant (p = 0.54, post-ANOVA Tukey-Kramer multiple comparison test). This indicates that there could be an asymmetrical development of functional connectivity which is observable in adult birds.

Functional connectivity increases in developing juveniles

A large-scale study in humans showed that maturation coincides with the increase of EEG functional connectivity and peaks at middle-age adulthood.[40] We investigated whether the avian brain of zebra finch shares similar patterns of connectivity during development. We have regressed intra- and inter-hemispheric correlations as a function of the birds' age. The regression function has the following exponential form: $Connectivity = A - B * exp(-age/\tau)$, where A and B are model parameters accounting for the initial point and the range of the exponential function and the time constant, τ, represents the time it takes for the connectivity to reach 63 % of the maximum.

The regression curves as well as the Pearson's r for a linear fit in the juvenile group are displayed in Figure 4A. The regression was calculated to fit the L-L, R-R, and L-R CCs to the juvenile age. In this calculation, we considered three passbands separately: the low frequency band (1.5-8 Hz), high frequency band (30-49 Hz), and full bands (1.5-200 Hz). Connectivity increased with maturation in most of the bands, with an average Pearson correlation of R = 0.35 ± 028 (mean ± SD, p=0.002, t-test); however, linear fits of the data were not statistically significant in all cases (see asterisks, Figure 4A). Specifically, we observed that connectivity in

L-L channels increased significantly in all bands, but that the R-R connectivity was not significant in any bands. The L-R connectivity was only significant when computed for the full band, but not the low or high bands.

Time constants arising from the exponential fit ranged from 33.3 to 100.0 days, demonstrating a fast increase of functional connectivity during development. We observed the highest rate of increase for the left hemisphere (L-L) pairs and for the inter-hemispheric (L-R) comparisons. In contrast, we did not observe a significant change of connectivity across age in adults ($p > 0.05$, t-test for correlation coefficient; data not shown). These findings support the hypothesis that the juvenile zebra finch brain undergoes rapid changes in connectivity that stabilize in adulthood, and which is in line with observations in human studies[40].

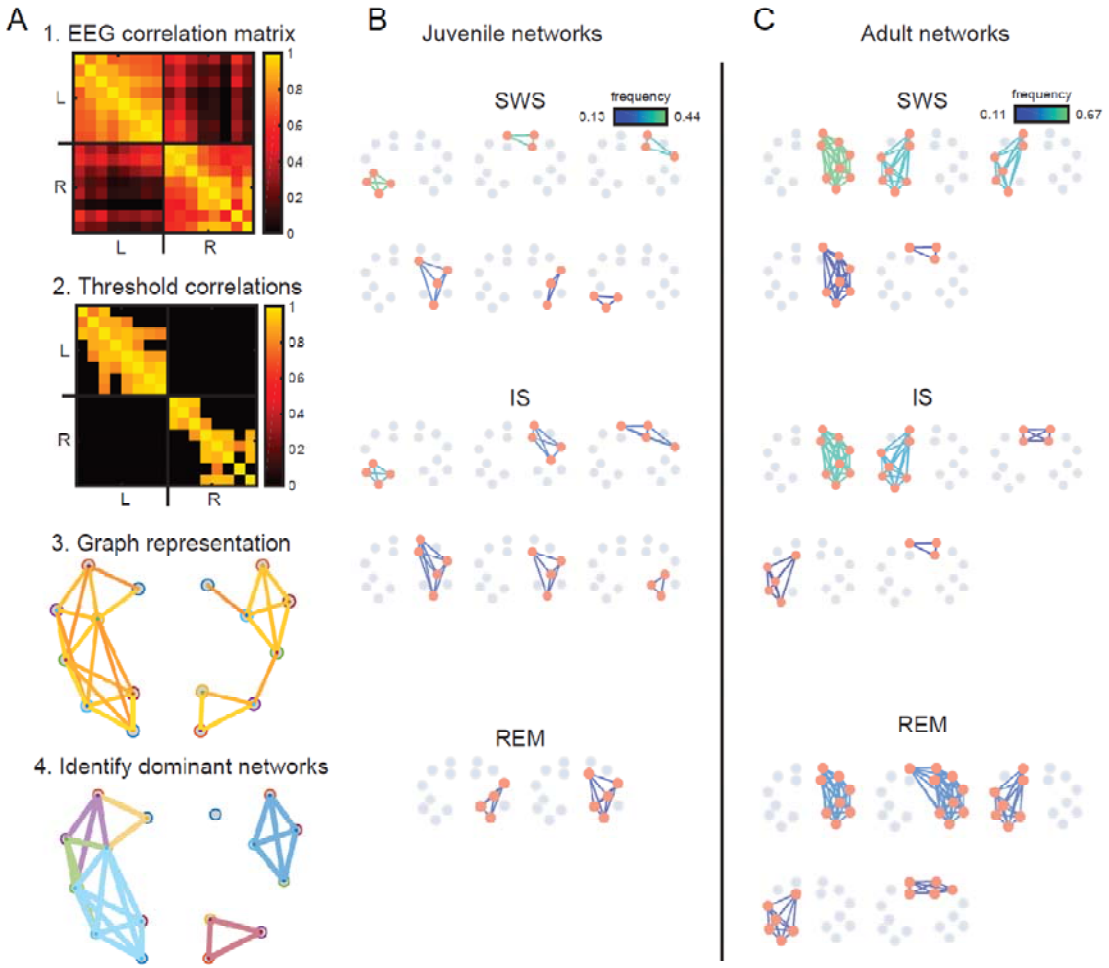

Figure 5 Graph theory analysis reveals larger networks of correlated EEG activity in adults compared to juveniles. (A) The main steps for the extraction of the highly-correlated networks are illustrated (see Methods for more details). 1- The EEG correlation matrix was computed for each 3-second bin. 2- Based on a statistical method,[41] significantly correlated pairs were kept for further analysis. 3- A graph representation of the significantly correlated pairs is constructed. To construct this graph, each EEG channel is represented by a node, and

a link connects two nodes for the case where the correlation between the corresponding EEG channels is significantly high. 4. Using the Bron-Kerbosch algorithm in graph theory,[42] we extracted the subnetworks for which all channels are highly correlated, i.e. dominant networks. The number and size of these networks is an indicator of functional connectivity pattern. (B) Dominant networks extracted from a juvenile during different stages of sleep across all nights. Juvenile is indicated as light brown in Figure 1E. (C) Dominant networks extracted from an adult during different stages of sleep. Adult is indicated as green in Figure 1E. Compared to juveniles, prominent networks are larger and less numerous in adults, an indication of stronger functional connectivity in adult birds. Color coding represents the frequency of occurrence for each network across bins, i.e. the fraction of bins where the network appeared. IS: intermediate stage.

Graph theory analysis reveals larger networks of correlated EEG activity in adults compared to juveniles.

In order to investigate how functional connectivity changes as a function of age, we used graph theory to identify dominant coactive networks in adults and juveniles (Methods; Figure 5A). Considering each recording site as a graph node, we analyze each 3-second bin of EEG, and connected a pair of channels with a link if their activity was significantly correlated (Methods). Then we extracted the subnetworks wherein each channel was highly correlated with all the other channels in the subnetwork. We only kept the subnetworks that appeared at least in 10% of the bins each night, for three nights. For simplicity we denote such a highly correlated subnetwork as a *dominant* network. Samples of these dominant networks are displayed in Fig. 5 for a juvenile (Figure 5B) and an adult (Figure 5C).

We analyzed the 8 out of 10 birds for which we had at least 3 nights of data (3 adults and 5 juveniles). In these birds, the size of dominant networks (the number of nodes), and their abundance (the number of dominant networks per bird), was used as an indication of overall connectivity. The average dominant network size was significantly larger for adults compared to juveniles (8.2 ± 2.9 channels (mean ± SD) for the adults and 4.2 ± 2.1 channels for the juveniles, $p = 3.0 \times 10^{-8}$, Wilcoxon rank-sum test). The total number of subnetworks that appeared for juveniles was slightly larger than for adults (on average 10.6 ± 4.6 dominant networks in the juveniles (n = 5) versus an average of 7.3 ± 4.6 for adults (n = 3). Therefore, the graph theory analysis reveals two distinct patterns of compartmentalization of neural activity in the adult and juveniles: the EEG activities tend to divide into a smaller number of large highly-correlated networks in the adult brain, and more numerous smaller subsets in the juvenile brain. This is another manifestation of the increased functional connectivity of the brain in the adult birds.

Discussion

Alteration of sleep architecture during development

Humans undergo drastic changes in sleep patterns during their lifetimes. Both the macro-level structure of sleep, i.e. total sleep time and organization of sleep stages, as well as the micro-level architecture of sleep, i.e. the brain oscillations of sleep, change as a function of age.[28]

In human development, children and adolescents spend more time in SWS. A meta-analysis of 65 articles published between 1960 and 2003 showed that in children, adolescents, and adults, the percentage of SWS was significantly negatively correlated with age. Similarly, a 5-year longitudinal study in children and adolescents revealed that non-REM delta and theta activity drops sharply at the age of 10 and continues to decline until the age of 16.[5] Tracking EEG slow-wave amplitude in combination with anatomical magnetic resonance imaging linked the reduction of slow waves with reduction of gray matter during the course of cortical maturation in adolescence.[49]

Age-related changes in sleep are not specific to humans, and have also been documented in animals ranging from rodents[6,50,51] to the fruit fly.[7] In the senescence-accelerated mouse, which is an accelerated-aging model, it has been demonstrated that aging deteriorates REM sleep architecture.[6] The genetic contribution to age-related changes in sleep has also been investigated using inbred mouse strains, concluding that most of sleep variables are age-dependent, although not necessarily varying with the age in a monotonic fashion.[51] In flies, it has been illustrated that age-dependent variations of sleep share similarities with that of humans and other mammals: not only do older flies have more fragmented sleep and reduced total sleep time compared to young flies, but older flies also fail to recover as much sleep after sleep deprivation.[7]

Although we were not able to quantify the total amount of time spent in SWS due to our use of the continuous DOS variable, we showed that DOS was significantly lower in adults compared to juveniles. Furthermore, we demonstrated that the reduction in DOS that we observed in adults was due to the reduction of power at low frequencies, and not due to an increase in gamma frequencies.

The reduction of SWS as a function of aging in both humans and zebra finches might indicate a common developmental function of SWS across mammals and birds. Specifically, SWS is known to have a critical role in the maintenance of memory in rodents,[52-54] and humans.[55-57] We hypothesize that SWS, or more generally slow oscillations, may have a similar role in memory consolidation in the avian brain. Indeed, a study in chicks found a significant dependency between imprinting memory consolidation and EEG theta oscillations during sleep and supports this hypothesis.[58] Additional investigations that leverage behavioral paradigms such as song learning [59-61] or spatial memory[62,63] could help us better understand the interplay between brain oscillations and different types of memory in the developing avian brain. Furthermore, our study investigated zebra finches that were older than 50 days post hatch (dph); the developmental changes that occur during early development in juvenile songbirds - and their similarities to human sleep development in early childhood - remain an open area of inquiry.

Local waves in human and rodent studies

The two global behavioral states of sleep, non-REM and REM stages, are distinguished by their unique neural signature.[10] However, recent studies have shown that cortical waves during non-REM sleep are not as global as previously thought.[64] Intracranial recordings in rodents,[65,66] and human,[32] have demonstrated that non-REM slow waves most often appear in a certain subset of brain regions for each wave, rather than occurring across all cortical areas in a synchronous manner. During human sleep, simultaneous scalp EEG, intracerebral EEG, and unit recordings

shows that most slow waves - as well as the accompanying active and inactive neuronal states - occur locally.[32]

Similarly, the understanding of awake-like, low-amplitude, high-frequency cortical activity during REM sleep has been challenged by the observance of local slow waves during REM in rodents:[64] Slow waves were regularly observed during REM, but only locally in primary sensory and motor cortical areas and mostly in layer 3 and 4.[64]

In our study, local waves were highly correlated with the amplitude of the DOS, but importantly, local waves were not absent during periods of low DOS (putative REM). Furthermore, in accord with the observations in humans,[28,32] the amplitude of the slow waves was higher in the anterior sites of the zebra finch brain as compared to posterior sites.

Overall, our observation of local waves in an avian brain, in accordance with rodent and human studies, supports the idea that sleep regulation could occur locally,[34,67] and that multiple local generators could contribute to the observed SWA in EEG.[36,68]

Functional connectivity in comparison with human and mammalian studies

In mammals, the corpus callosum heavily interconnects the right and left cortical hemispheres. The inter-hemispheric connections in birds are far fewer and the telencephalic pallium sensory-motor and associative regions receive limited input from the contralateral hemisphere.[69,70] The only inter-hemispheric pathways at the telencephalic level in birds consist of anterior commissure and the much smaller hippocampal commissure .[69]

In addition, the great majority of pallial areas do not participate by themselves in inter-hemispheric exchange in the avian brain.[69] Instead, commissural exchange rests on a rather small arcopallial and amygdaloid cluster of neurons.[69] In comparison, in the eutherian mammals which includes humans and rodents, the cingulate cortex and most of isocortex are connected to the contralateral homotopic regions via abundant interhemispheric corpus callosum tracts.[71]

However, it is worth noticing that the lower inter-hemispheric connectivity in the avian brain is not necessarily a disadvantage compared with placental mammals. For instance, unihemispheric sleep, which is observed in many bird species,[21,72-79] including zebra finch,[1] helps the bird overcome the problem of sleeping in risky environment,[74] and might be facilitated through weaker interhemispheric connectivity. If that is true, we should expect a smaller relative size of corpus callosum in cetacean mammals, as they also express unihemispheric sleep, which is indeed the case; callosal area to brain mass ratio is smaller in cetacians compared to other mammalian groups possessing a corpus callosum.[80,81] Another indication of more independent hemispheres, that might be related to the absence of corpus callosum, is independent eye movements enabling birds to scan,[82] and focus,[83] upon different environmental stimuli simultaneously.

In this work, we showed that the inter-hemispheric functional connectivity is almost half of the intra-hemispheric connectivity, and this observation was true in both juveniles and adults. This lower inter-hemispheric functional connectivity could be explained by considering the confined

commissural bundles in the avian brain. A large MRI study of brain connectivity over 123 mammalian species, including some species without corpus callosum, revealed a connectivity conservation law: that is, species with highly connected hemispheres appear to have weaker inter-hemispheric connections.[84] This trade-off between inter-hemispheric and intra-hemispheric connectivity was also observed in a large-scale human study.[85]

Since maintaining a normal level of functional connectivity is essential for the brain to function properly,[86-89] we hypothesize that in birds, the evolution of brain connectivity took an alternative path in contrast with the emergence of corpus callosum in placental mammals; namely, that the left and right hemispheres developed stronger intra-hemispheric connectivity to compensate the lower inter-hemispheric connectivity while maintaining higher levels of hemispheric autonomy. This hypothesis is in agreement with higher telencephalic neuronal density, i.e. ratio of telencephalic neurons to brain mass, in birds compared to mammals, including primates. However, more rigorous verification of this hypothesis would require further studies of functional connectivity in combination with brain stimulation to simultaneously measure effective connectivity, similar to human studies.[90,91] Further research into the avian brain connectivity is also encouraged by the emerging clinical literature signifying the importance of functional connectivity measures,[87,92] particularly since it could be achieved via non-invasive imaging techniques like functional MRI (fMRI),[93-96].

Cerebral asymmetries in non-mammalian species

Handedness and cerebral asymmetry were believed to be uniquely human; [97] however, this idea is being reevaluated due to the accumulating observations of behavioral asymmetries in non-human species, including animal behaviors such as turning direction to attack the prey, preferred direction for feeding, or the asymmetric control of mouth structures in vocalization.[97-102]

In mammals, asymmetries in vocalization apply to perception as well as to production. A left-hemispheric advantage for the perception of species-specific vocalizations has been observed in mice, rhesus monkeys, and Japanese macaques.[97] It has been speculated that these asymmetries may be precursors to left cerebral dominance for language processing in humans.[97] A longitudinal fMRI study in human infants revealed a rapid rise of interhemispheric connectivity in the language regions, peaking at ~11.5 months of age, indicating an initial rise of interhemispheric connectivity followed by a decline and transition toward asymmetry in the second year. This shift was accompanied by an increase in the functional connectivity of these regions within the left hemisphere.[103] In general, a higher correlations between language areas in the left hemisphere than between their right hemisphere homologues have been reported in human adults.[104]

In zebra finches, hemispheric dominance has also been demonstrated. Similar to findings in humans, the neuronal activation after initial exposure to a song (or speech) is documented to be bilateral,[105] and hemispheric dominance develops with vocal proficiency.[106] Similar to this left-lateralized auditory system, right-lateralization of visual processing has also been reported in zebra finches.[101]

In summary, in this study, we observed that the functional connectivity is stronger in adult zebra finches than in the juveniles, and that it grows during the development. To which extent this growth in functional connectivity is related to structural connectivity, i.e. neuroanatomical developments, is an open question. Moreover, whether the stronger and hemispherically dominant connectivity that forms at the end of maturation period is a requirement for the development of song system, or is just a direct consequence of brain maturation, remains to be investigated.

Sleep stage as a continuous variable

It is well documented that the EEG activity during sleep in birds includes stages that mimic mammalian REM and SWS.[1] However, this does not necessarily mean that the avian brain switches discretely between these stages. At least in the zebra finch[1] and budgerigar,[2] the brain undergoes oscillatory activity that is neither SWS nor REM. This so-called 'intermediate' stage (IS) has been compared to the non-REM stages 1 and 2 in mammals.[1]

The approach to categorization EEG activity into REM and non-REM sleep stages stems from comparison with the mammalian sleep and a pressure to emphasize similarities between the studied organism and adult mammals.[43] This categorization, although insightful, has the potential to bias an investigation into the dynamics of sleep in other (non-mammalian) animals. Indeed, even early studies in cat suggested "a progression from slow wave sleep to activated sleep and to activated sleep with rapid eye movements, rather than dichotomous states."[13] Even in the case of human sleep, the limitations of discrete sleep scoring have been critically discussed and alternative strategies for sleep analysis have been promoted.[44,45,46]

Therefore, in this study, we tried to avoid the categorization of sleep into separate stages, and instead used a continuous variable, the *depth of sleep* (DOS), to quantify sleep dynamics. This method is analogous to methods used in rodents[30,47,48] and cat[29], but accounts for the dominant frequency bands observed during avian sleep.[1,2] While this low-to-high frequency ratio better reflects the continuity of EEG oscillations during sleep, it still enabled us to compare the results with the traditional sleep-staging studies, since SWS and REM stages appear at the high and low extremes of the DOS variable, respectively.

Acknowledgments

This research was funded by grants from the German Research Foundation (Deutsche Forschungsgemeinschaft; ON 151/1-1) and the Daimler and Benz Foundation (Postdoctoral scholarship) to J.M.O. The authors are grateful to B. Seibel and Y. Schwarz for technical assistance; C. Fink and E. Jochen for help with mechanical design, fabrication, and electronics; A. Schuhbauer for administrative assistance, and H. Luksch, U. Firzlaff, T. Fenzl, and M. Shein-Idelson for feedback on previous versions of the manuscript.

Author contributions

	HY	JMO
Conceptualization		■
Methodology	■	■
Software	■	■
Validation		■
Formal Analysis	■	
Investigation	■	
Writing – original draft	■	
Writing – reviewing & editing	■	■
Funding acquisition		■
Resources		■
Visualization	■	■
Supervision		■
Project Administration		■

Declaration of interests

The authors declare no competing interests.

Methods

Data and code availability

All data reported in this paper will be shared by the lead contact upon request.

Experimental animals

We used 3 adult and 7 juvenile zebra finches in these experiments. Zebra finches reach their sexual maturation at around 90 days post hatch (dph). The sex and the age of the birds at the first recording night are summarized in Table. 1.

Bird name	sex	age (dph)	Number of good electrodes
W009	m	50	15
W016	f	50	13
W020	m	53	16

W018	f	51	14
W021	f	52	13
W043	m	69	15
W041	m	69	15
73-03	m	686	16
72-00	m	764	14
72-94	m	780	15

Table 1 **Description of experimental birds used in this study.** Bird name, sex, age in days post hatch (dph) at the first night of recording, and number of non-noisy electrodes recorded in the zebra finch is indicated. Table follows the same order as the data displayed in Figure 1E.

Prior to experiments, birds were housed on site in volieres and were kept on a 12:12-hr light:dark cycle. Finches received seed mix, millet, sepia bone, and water *ad libitum* and were given fresh salad and cooked egg supplements once a week.

All experiments were carried out in accordance with Oberbayern, German, and European laws on animal experimentation (Approval #ROB-55.2-2532.Vet_02-18-108: J.M.O.).

Behavior and video acquisition

Zebra finches were acclimated to the recording chamber for at least 5 days prior to the experiments. Experimental animals were kept together with a non-experimental female bird (adults) or the father tutor bird (juveniles) to prevent social isolation. Birds were separated from each other with a clear Plexiglas panel, such that animals could hear and see each other but could not interact physically.

In the recording chamber, finches received seed mix, millet, sepia bone, and water *ad libitum*. The recording chamber (total inner measurements: 120 cm x 50 cm x 50 cm) was equipped with LED lights, a UV bird light (Bird Systems, Germany), an infrared (IR) LED panel (850 nm), and had continuous air circulation. Video footage of the experimental animal was acquired with a near-IR sensitive camera (acA1300-60gm, Basler Ag, Germany) with custom-written software (ZR View, Robert Zollner) at a frame-rate of 20 fps, triggered with a pulse generator (Pulse Pal, Sanworks, NY, USA,[107]).

Electrode preparation and positioning

For each experiment, we constructed silver ball EEG electrodes from silver wire (254 µm bare wire diameter, Science Products GmbH, Hofheim, Germany) by melting the tip of the wire into a smooth ball of approximately 0.50 mm in diameter using a Bunsen burner (CFH Löt- und Gasgeräte GmbH, Offenau, Germany). 18 electrodes were implanted: 8 electrodes were implanted over each hemisphere, and 2 additional ground and reference electrodes were implanted over the cerebellum (Figure 1A). Electrode sites varied slightly across adult birds to avoid superficial blood vessels (variation less than 0.5 mm). The adult electrode map was rescaled for juveniles due to difference in head size, in order to maintain the relative electrode spacing.

Anesthesia and Surgery

Zebra finches were anesthetized with isoflurane (1-3 %) mixed with oxygen generated with an oxygen concentrator (EverFlo OPI, Phillips, Netherlands) and administered using a vaporizer

(Isotec 4, Groppler, Germany) through a small tube directly into the beak of the bird. Excess isoflurane was collected and filtered (Scavenger LAS, Groppler, Germany). The body temperature was monitored with an infrared thermometer (EVENTEK E300, ShenZhen ShengYa Hardware Produts Co, China), and maintained at above 39.5°C through the use of a homoeothermic heating pad (Harvard apparatus, MA, USA).

Under anesthesia, the experimental animal was positioned in a small animal stereotaxic frame (Kopf Instruments, CA, USA). The scalp was anesthetized with xylocaine (Xylocain Pumpspray, Aspen Pharma Trading Limited, Ireland), the feathers were removed with forceps, and the scalp was resected along the midline. For each EEG electrode, a small hole was drilled above the forebrain with a high speed dental drill (Volvere i7, NSK Europe GmbH, Germany). EEG electrodes were placed in the sites and secured using dental cement (Paladur, Henry Schein Dental, Germany).

Following surgery, the animal was released from the stereotaxic frame and administered a dose of Metamizol (100-150 mg/kg, i.m.). The animal remained on a heating pad until full recovery from anesthesia. An antibiotic (Baytril, 1025 mg/kg, i.m.) and an analgesic (Carprofen, 4 mg/kg, i.m.) were administered up to 3 days post-operatively. Following recovery from surgery, the animal returned to entirely normal feeding, sleeping, and singing behaviors as observed before surgery.

Overnight electrophysiological recordings

Recordings were started at the second night after the implantation. One hour before lights off (light off period: 9:00 PM - 9:00 AM), the animal was connected to the headstage and custom-made lightweight tether cable and allowed to assume a natural sleep posture on a branch that had been placed on the floor of the chamber. The camera was positioned to allow for the best visualization of the animal during sleep. The animal was allowed to sleep naturally overnight, and was disconnected from the headstage and tether cable shortly after lights turned on. Data from the first night after surgery was not used in the analysis.

The EEG electrodes were connected to a preamplifier (Intan Technologies, RHD2132), which was connected to the data acqu.sition board via the tether cable. Recordings were performed with an Open Ephys acquisition board (Open Ephys Production Site, Portugal; [108]). Recordings were grounded and referenced against one of the reference wires. Signals were sampled at 30 kHz, wide band filtered (0.1-9987 Hz), and saved in a continuous format using the Open Ephys GUI. [108]

Anatomy

After the period of recording was over, the animal was deeply anesthetized with an overdose of sodium pentobarbitol (250 mg/kg, i.m.) until the corneal reflex disappeared. Afterward, the animal was decapitated, the brain was removed from the skull and post-fixed in 4% paraformaldehyde in PBS for postmortem verification of electrode sites.

Data Analysis

Video Motion Extraction

We developed a program in MATLAB (The MathWorks Inc., Natick, MA, USA) to extract a single variable that represents the overall amount of frame-by-frame movements. For each 2 consequent frames ($m \times n$ matrices containing gray-scale pixel values), we first computed the absolute value of the difference (eq. 1).

$$diff(k)_{m,n} = \left| frame(k)_{m,n} - frame(k-1)_{m,n} \right| \qquad (1)$$

where k represents the frame number. $diff(k)_{m,n}$ will have a non-zero value at any pixel that has changed from frame $k-1$ to frame k. Then we extract the weighted average of $diff(k)_{m,n}$ along the x and y axes separately. For example for the weighted average along the x axis, we sum up the $diff(k)_{m,n}$ values along the rows and then scale it by the vector $[1\ 2 \ldots n]$, the x vector, (eq. 2).

$$x = [1\ 2 \ldots n]', \quad S = sum(diff(k).,1) \times x \qquad (2)$$

S_y is acquired in the same way. At the end, using pythagoras formula, we merge Sx and Sy to achieve the total magnitude of movement (eq. 3).

$$Movement(k) = \sqrt{{S^2}_x + {S^2}_y} \qquad (3)$$

EEG preprocessing and DOS analysis

EEG was down-sampled by a factor of 64 (final sampling rate: 468.75 sps). Each channel was normalized (using the MATLAB “z-score” function) to avoid inhomogeneities that might arise from changes in the impedance of electrodes over days and binned into 3-second windows.

Sleep was behaviorally defined based on movement extracted from the video data. Bins where the movement was above its median by 2 interquartile intervals were labeled as awake and consequently excluded from analysis. This automatic sleep/wake labeling was validated on one data set that was that was also labeled visually as ground truth. Additional bins were excluded for which the EEG amplitude was more than 4 interquartile intervals above the zero base line. In total, approximately 400, 3-s bins (or 20 minutes of data, or less than 3%) were discarded per night of recording due to artifact rejection. Finally, some channels were broken and were therefore excluded from all further analysis. The number of used electrodes for each bird is reported in Table 1.

We assessed the sleeping brain dynamics not in discrete stages, but as a continuous variable, the “depth of sleep” (DOS). DOS was defined as the ratio of power in delta and theta bands (1.5 - 8 Hz) over the power in low gamma (30 - 49 Hz). Spectral power was computed using the Multitaper method with the time-halfbandwidth product equal to 1.25 and the number of DFT points equal to 2048.

Sleep stage identification

Previous research in zebra finch sleep shows that each stage of sleep, i.e. SWS, IS, or REM are computed based on their gamma- and delta-power content.[1] That means, for example, SWS bins contain the highest delta power, REM the lowest, and the IS bins stand in between.

Therefore, in order to include samples from different stages of sleep, we first ordered the EEG bins according to their DOS value. The highest 10 percent were considered SWS, the lowest 10 percent as REM, and the 10 percent of the data encompassing the median DOS formed the IS group.

Stage transition detection

In order to detect the number of transitions from SWS to REM, we used a moving threshold calculated over 30-minute windows of the non-smoothed DOS values. The SWS threshold was defined as the moving average plus 0.4 × moving iqr (calculated over 30-minute windows), and the threshold for REM was defined as the moving average minus 0.4 × moving iqr.

Detection of local waves

Normalized EEG data was filtered using a band-pass filter (0.5 - 20 Hz) to suppress the high frequency components that might affect the precise localization of wave peaks and troughs. Local wave detection consists of two steps: (1) detection of all the wave peaks or troughs across all the channels, and (2) extraction of the simultaneously-occurring waves.

All positive or negative peaks that were more than one inter-quartile interval away from median were detected. To prevent the double-detection of waves with a negative deflection following the positive peak, or vice versa, we set a minimum inter-wave period of 90 ms where subsequent peaks were not detected. We only considered peaks detected across different channels which occurred within a 10 ms time widow as simultaneous. Finally, in order to be considered a *local* wave, a wave needs to be present in only a subset of all the channels. Here we considered the simultaneous observation of peaks across the channels as a local wave if the peaks were present in at least 4 channels (25%) and not more than 12 channels (75%).

Connectivity analysis

In order to have a measure of intra-hemispheric EEG correlation, we averaged the correlations between all pairs of right hemisphere channels (R-R; numbering 15, 21, or 28 pairs of channels, corresponding to 6, 7, or 8 non-noisy channels on the right hemisphere) and all pairs of left hemisphere channels (L-L; numbering 21 or 28 pairs of channels, corresponding to 7 or 8 non-noisy channels on the left hemisphere). The inter-hemispheric connectivity was computed as the average of the correlation between the pair of channels from opposing hemispheres (42-64 pairs, depending on the number of non-noisy channels). This correlation analysis was performed separately for the adult and juvenile group, and for 3 different frequency bands: low frequency (1.5-8 Hz), gamma (30-49 Hz), and full band (1.5-200 Hz)

Graph theory analysis

We explored the compartmentalization of brain activity by extracting *dominant* subnetworks of activity using methods from graph theory. We define a dominant subnetwork as a subset of EEG channels wherein (1) each pair of channels are significantly correlated and (2) it has the maximum number of such channels, i.e., no other channel could be added that correlates highly with the current channels. For example, if there are 4 EEG channels which are mutually highly-correlated with each other, and no other channel exists which is highly correlated with all of these 4 channels, then these 4 channels form a dominant subnetwork. Such a subnetwork is called a “clique” in graph theory literature.

We extracted dominant subnetworks for each stage of sleep separately. First, we computed the pair-wise correlation matrix for each 3-second bin belonging to the given sleep stage (e.g., REM, SWS, or IS) for all channels. From the correlation matrix, the statistically significant correlated pairs of channels were extracted using a statistical inference technique.[41] A MATLAB implementation of this method was provided by the authors of [41]. Having the significantly correlated pairs of EEG, the cliques were extracted using a MATLAB implementation of the Bron-Kerbosch algorithm.[109] Among the obtained dominant subnetworks, we discarded the ones involving fewer than 3 EEG channels and appearing in fewer than 10% of the bins for that sleep stage. In the end, for all the recording nights of a given bird, we kept the subnetworks that were consistent across all the recording nights in a given sleep stage. The size of these dominant subnetworks, i.e. number of EEG channels involved, and number of these subnetworks were reported.

Supplementary Figures

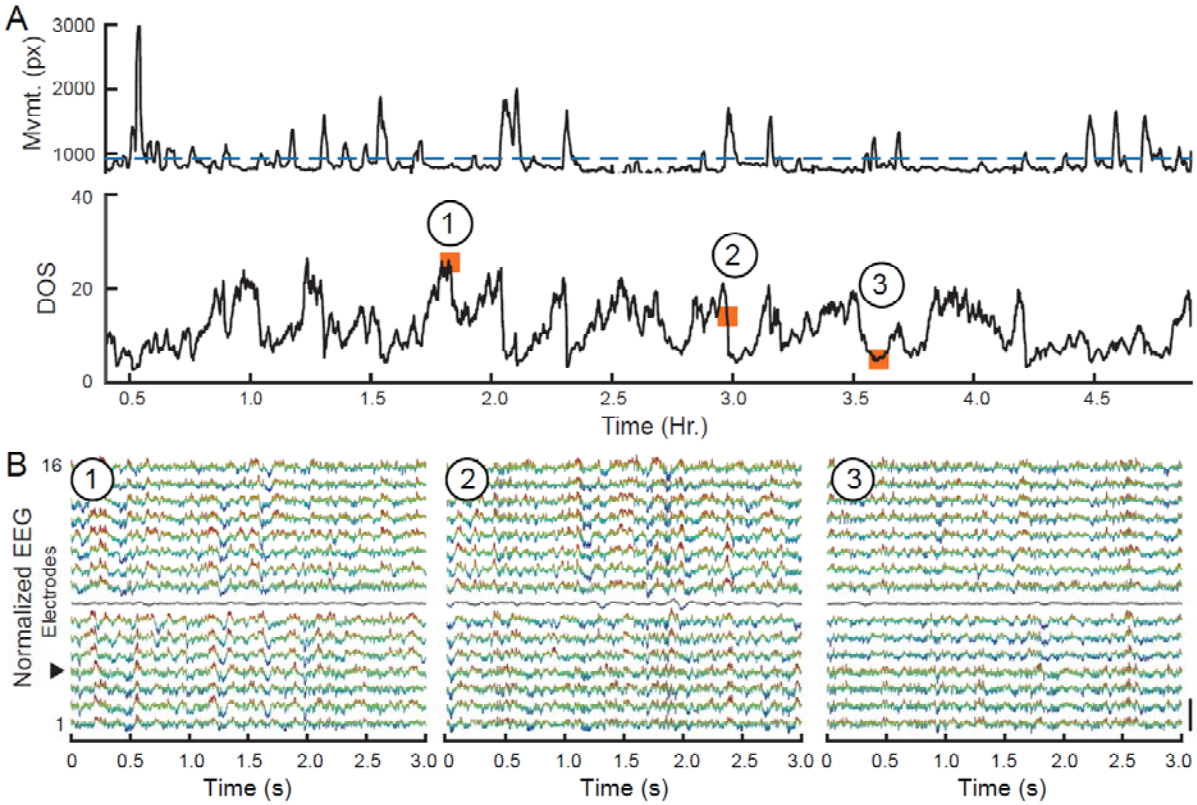

Figure S1. Sleep EEG and corresponding DOS in a juvenile. (A) Top: Movement extracted from the infrared video recording (px, pixels). Blue line is the threshold delineating wake/sleep. Bottom: Corresponding DOS ratio shows the fluctuations in the oscillatory components of EEG. Movement and DOS smoothed with a 30-secs window for visualization purposes. Orange squares 1, 2, and 3, correspond to EEG data in C. (B) 3-s examples of EEG from SWS, IS, and REM sleep, respectively.

Color scheme is for visualization purposes only. Similar to adult data (in Fig. 1), EEG recordings show distinct patterns across stages. DOS was calculated from the EEG recorded on channel 4. Channel 8 (grey line) was noisy and discarded in further analysis.

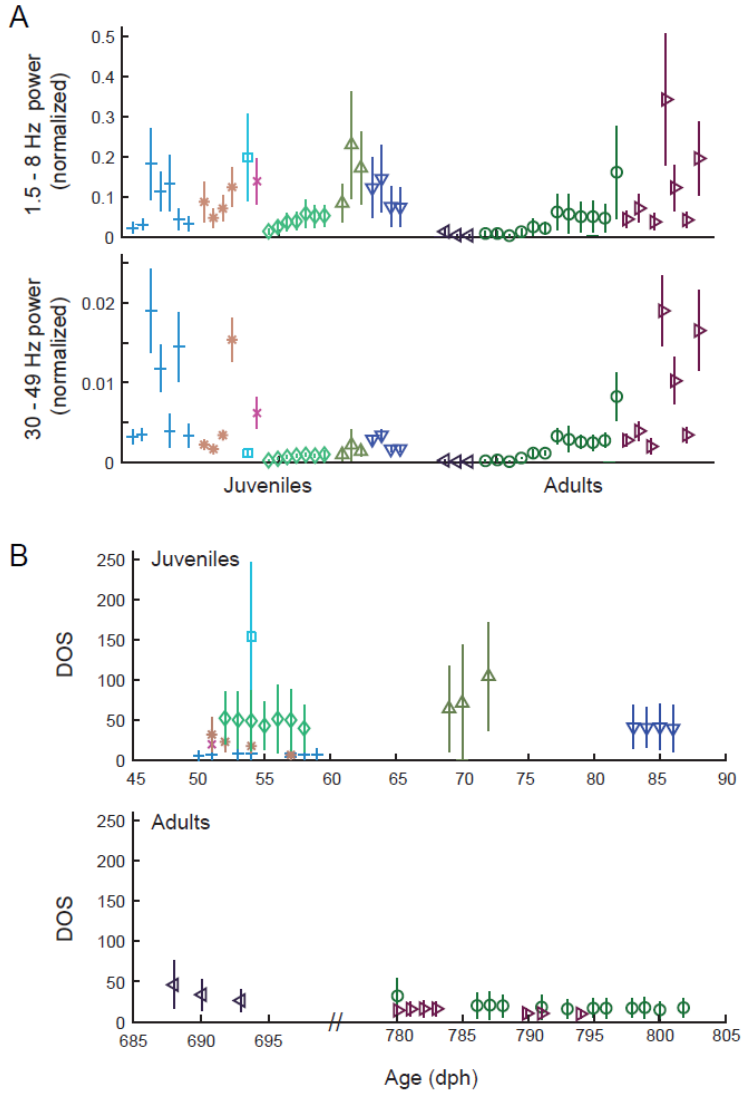

Figure S2. Low and high frequency power across groups, and DOS versus actual age. (A) DOS was significantly larger in juveniles compared to adults. To see whether this difference in DOS was due to the difference in the low frequencies band or the gamma band, we compared the power in each of these bands across juvenile and adult groups. The relative power in gamma band was the same across the groups (0.0040 ± 0.0050 in juveniles and 0.0038 ± 0.0052 in adults, mean ± SD, scale-free due to relative power, p-value = 0.55, Wilcoxon rank-sum test). However, the relative power in the low-frequencies was significantly higher in the juveniles than in adults (0.88 ± 0.059 in juveniles and 0.062 ± 0.080 in adults, p-value = 0.02, Wilcoxon rank-sum test). This suggests that the Delta and Theta oscillatory components of EEG, i.e. 1.5 - 8 Hz waves are lower in adults. (B) DOS is plotted as a function of the age in juvenile birds (upper plot) and adults (lower plot). DOS is generally consistent across nights for each single bird, but a large variability was observed across birds.

References

1. Steven Low, P., Shank, S.S., Sejnowski, T.J., and Margoliash, D. (2008). Mammalian-like features of sleep structure in zebra finches.
2. Canavan, S.V., and Margoliash, D. (2020). Budgerigars have complex sleep structure similar to that of mammals. PLoS Biology *18*. 10.1371/journal.pbio.3000929.
3. Lesku, J.A., Vyssotski, A.L., Martinez-Gonzalez, D., Wilzeck, C., and Rattenborg, N.C. (2011). Local sleep homeostasis in the avian brain: convergence of sleep function in mammals and birds? Proceedings of the Royal Society B: Biological Sciences *278*, 2419-2428.
4. Rattenborg, N.C., and Martinez-Gonzalez, D. (2015). Avian versus mammalian sleep: the fruits of comparing apples and oranges. Current Sleep Medicine Reports *1*, 55-63.
5. Campbell, I.G., and Feinberg, I. (2009). Longitudinal trajectories of non-rapid eye movement delta and theta EEG as indicators of adolescent brain maturation. Proceedings of the National Academy of Sciences *106*, 5177-5180.
6. Colas, D., Cespuglio, R., and Sarda, N. (2005). Sleep wake profile and EEG spectral power in young or old senescence accelerated mice. Neurobiology of Aging *26*, 265-273. https://doi.org/10.1016/j.neurobiolaging.2004.03.004.
7. Vienne, J., Spann, R., Guo, F., and Rosbash, M. (2016). Age-Related Reduction of Recovery Sleep and Arousal Threshold in Drosophila. Sleep *39*, 1613-1624. 10.5665/sleep.6032.
8. Anafi, R.C., Kayser, M.S., and Raizen, D.M. (2019). Exploring phylogeny to find the function of sleep. Nature Reviews Neuroscience *20*, 109-116. 10.1038/s41583-018-0098-9.
9. Nath, R.D., Bedbrook, C.N., Abrams, M.J., Basinger, T., Bois, J.S., Prober, D.A., Sternberg, P.W., Gradinaru, V., and Goentoro, L. (2017). The Jellyfish Cassiopea Exhibits a Sleep-like State. Current Biology *27*, 2984-2990.e2983. 10.1016/j.cub.2017.08.014.
10. McCarley, R.W., and Sinton, C.M. (2008). Neurobiology of sleep and wakefulness. Scholarpedia.
11. Kashiwagi, M., and Hayashi, Y. (2020). The existence of two states of sleep as a common trait in various animals and its molecular and neuronal mechanisms. Current Opinion in Physiology. Elsevier Ltd.
12. Yamazaki, R., Toda, H., Libourel, P.A., Hayashi, Y., Vogt, K.E., and Sakurai, T. (2020). Evolutionary Origin of Distinct NREM and REM Sleep. Front Psychol *11*, 567618. 10.3389/fpsyg.2020.567618.
13. Sterman, M., Knauss, T., Lehmann, D., and Clemente, C. (1965). Circadian sleep and waking patterns in the laboratory cat. Electroencephalography and clinical Neurophysiology *19*, 509-517.
14. Saper, C.B., Fuller, P.M., Pedersen, N.P., Lu, J., and Scammell, T.E. (2010). Sleep state switching. Neuron *68*, 1023-1042.
15. Shein-Idelson, M., Ondracek, J.M., Liaw, H.-P., Reiter, S., and Laurent, G. Slow waves, sharp waves, ripples, and REM in sleeping dragons. https://www.science.org.
16. Leung, L.C., Wang, G.X., Madelaine, R., Skariah, G., Kawakami, K., Deisseroth, K., Urban, A.E., and Mourrain, P. (2019). Neural signatures of sleep in zebrafish. Nature *571*, 198-204. 10.1038/s41586-019-1336-7.
17. Libourel, P.-A., Barrillot, B., Arthaud, S., Massot, B., Morel, A.-L., Beuf, O., Herrel, A., and Luppi, P.-H. (2018). Partial homologies between sleep states in lizards, mammals, and birds suggest a complex evolution of sleep states in amniotes. PLoS biology *16*, e2005982.
18. Iglesias, T.L., Boal, J.G., Frank, M.G., Zeil, J., and Hanlon, R.T. (2019). Cyclic nature of the REM sleep-like state in the cuttlefish Sepia officinalis. Journal of Experimental Biology *222*. 10.1242/jeb.174862.
19. Tainton-Heap, L.A.L., Kirszenblat, L.C., Notaras, E.T., Grabowska, M.J., Jeans, R., Feng, K., Shaw, P.J., and van Swinderen, B. (2021). A Paradoxical Kind of Sleep in Drosophila melanogaster. Current Biology *31*, 578-590.e576. https://doi.org/10.1016/j.cub.2020.10.081.

20. Alphen, B.v., Semenza, E.R., Yap, M., Swinderen, B.v., and Allada, R. (2021). A deep sleep stage in Drosophila with a functional role in waste clearance. Science Advances *7*, eabc2999. doi:10.1126/sciadv.abc2999.
21. Tobler, I., and Borbély, A.A. (1988). Sleep and EEG spectra in the pigeon (Columba livia) under baseline conditions and after sleep deprivation. Journal of Comparative Physiology A *163*, 729-738.
22. Rattenborg, N.C., Voirin, B., Cruz, S.M., Tistdale, R., Dell'Omo, G., Lipp, H.-P., Wikelski, M., and Vyssotski, A.L. (2016). Evidence that birds sleep in mid-flight. Nature communications *7*, 1-9.
23. Heller, H.C., Graf, R., and Rautenberg, W. (1983). Circadian and arousal state influences on thermoregulation in the pigeon. American Journal of Physiology-Regulatory, Integrative and Comparative Physiology *245*, R321-R328.
24. Šušić, V.T., and Kovačević, R.M. (1973). Sleep patterns in the owl Strix aluco. Physiology & Behavior *11*, 313-317.
25. Saucier, D., and Astic, L. (1975). Polygraphic study of sleep in young chickens at hatching, evolution at third and fourth days. Electroencephalography & Clinical Neurophysiology.
26. Szymczak, J.T. (1987). Distribution of sleep and wakefulness in 24-h light-dark cycles in the juvenile and adult magpie, Pica pica. Chronobiologia.
27. Scriba, M.F., Ducrest, A.-L., Henry, I., Vyssotski, A.L., Rattenborg, N.C., and Roulin, A. (2013). Linking melanism to brain development: expression of a melanism-related gene in barn owl feather follicles covaries with sleep ontogeny. Frontiers in zoology *10*, 1-12.
28. Mander, B.A., Winer, J.R., and Walker, M.P. (2017). Sleep and human aging. Neuron *94*, 19-36.
29. Mukovski, M., Chauvette, S., Timofeev, I., and Volgushev, M. (2007). Detection of active and silent states in neocortical neurons from the field potential signal during slow-wave sleep. Cerebral cortex *17*, 400-414.
30. Cape, E.G., and Jones, B.E. (1998). Differential modulation of high-frequency γ-electroencephalogram activity and sleep–wake state by noradrenaline and serotonin microinjections into the region of cholinergic basalis neurons. Journal of Neuroscience *18*, 2653-2666.
31. Buckelmüller, J., Landolt, H.P., Stassen, H.H., and Achermann, P. (2006). Trait-like individual differences in the human sleep electroencephalogram. Neuroscience *138*, 351-356. 10.1016/j.neuroscience.2005.11.005.
32. Nir, Y., Staba, R.J., Andrillon, T., Vyazovskiy, V.V., Cirelli, C., Fried, I., and Tononi, G. (2011). Regional Slow Waves and Spindles in Human Sleep. Neuron *70*, 153-169. 10.1016/j.neuron.2011.02.043.
33. Mascetti, G.G. (2016). Unihemispheric sleep and asymmetrical sleep: Behavioral, neurophysiological, and functional perspectives. Nature and Science of Sleep. Dove Medical Press Ltd.
34. Huber, R., Felice Ghilardi, M., Massimini, M., and Tononi, G. (2004). Local sleep and learning. www.nature.com/nature.
35. Massimini, M., Huber, R., Ferrarelli, F., Hill, S., and Tononi, G. (2004). The sleep slow oscillation as a traveling wave. Journal of Neuroscience *24*, 6862-6870. 10.1523/JNEUROSCI.1318-04.2004.
36. Murphy, M., Riedner, B.A., Huber, R., Massimini, M., Ferrarelli, F., Tononi, G., and Raichle, M.E. (2009). Source modeling sleep slow waves. www.pnas.orgcgidoi10.1073pnas.0807933106.
37. Simor, P., van der Wijk, G., Gombos, F., and Kovács, I. (2018). The paradox of Rapid Eye Movement sleep in the light of oscillatory activity and functional synchronization during phasic and tonic microstates. bioRxiv. 10.1101/498212.
38. Siclari, F., and Tononi, G. (2016). Local aspects of sleep and wakefulness. http://www.elsevier.com/open-access/userlicense/1.0/.
39. Bastos, A.M., and Schoffelen, J.M. (2016). A tutorial review of functional connectivity analysis methods and their interpretational pitfalls. Frontiers in Systems Neuroscience. Frontiers Research Foundation.
40. Smit, D.J.A., Boersma, M., Schnack, H.G., Micheloyannis, S., Boomsma, D.I., Hulshoff Pol, H.E., Stam, C.J., and de Geus, E.J.C. (2012). The brain matures with stronger functional connectivity and decreased randomness of its network. PloS one *7*. 10.1371/journal.pone.0036896.

41. Kramer, M.A., Eden, U.T., Cash, S.S., and Kolaczyk, E.D. (2009). Network inference with confidence from multivariate time series. Physical Review E *79*, 061916-061916-061913.
42. Bron, C., and Kerbosch, J. (1973). Algorithm 457: finding all cliques of an undirected graph. Communications of the ACM *16*, 575-577.
43. Blumberg, M.S., Lesku, J.A., Libourel, P.-A., Schmidt, M.H., and Rattenborg, N.C. (2020). What Is REM Sleep? Current Biology *30*, R38-R49. https://doi.org/10.1016/j.cub.2019.11.045.
44. Schulz, H. (2008). Rethinking sleep analysis: Comment on the AASM manual for the scoring of sleep and associated events. Journal of Clinical Sleep Medicine *4*, 99-103.
45. Guo, D., Thomas, R.J., Liu, Y., Shea, S.A., Lu, J., and Peng, C.-K. (2022). Slow wave synchronization and sleep state transitions. Scientific Reports *12*, 7467. 10.1038/s41598-022-11513-0.
46. Stevner, A.B.A., Vidaurre, D., Cabral, J., Rapuano, K., Nielsen, S.F.V., Tagliazucchi, E., Laufs, H., Vuust, P., Deco, G., Woolrich, M.W., et al. (2019). Discovery of key whole-brain transitions and dynamics during human wakefulness and non-REM sleep. Nature Communications *10*, 1035. 10.1038/s41467-019-08934-3.
47. Siapas, A.G., and Wilson, M.A. (1998). Coordinated interactions between hippocampal ripples and cortical spindles during slow-wave sleep. Neuron *21*, 1123-1128.
48. O'Keefe, J. (1976). Place units in the hippocampus of the freely moving rat. Experimental neurology *51*, 78-109.
49. Buchmann, d., Ringli, M., Kurth, S., Schaerer, M., Geiger, A., Jenni, O.G., and Huber, R. (2010). EEG Sleep Slow-Wave Activity as a Mirror of Cortical Maturation. Cerebral Cortex *21*, 607-615. doi:10.1093/cercor/bhq129.
50. Ingram, D.K., London, E.D., and Reynolds, M.A. (1982). Circadian rhythmicity and sleep: effects of aging in laboratory animals. Neurobiology of aging *3*, 287-297.
51. Hasan, S., Dauvilliers, Y., Mongrain, V., Franken, P., and Tafti, M. (2012). Age-related changes in sleep in inbred mice are genotype dependent. Neurobiology of Aging *33*, 195.e113-195.e126. https://doi.org/10.1016/j.neurobiolaging.2010.05.010.
52. Barnes, D.C., and Wilson, D.A. (2014). Slow-wave sleep-imposed replay modulates both strength and precision of memory. Journal of Neuroscience *34*, 5134-5142.
53. Oyanedel, C.N., Binder, S., Kelemen, E., Petersen, K., Born, J., and Inostroza, M. (2014). Role of slow oscillatory activity and slow wave sleep in consolidation of episodic-like memory in rats. Behavioural Brain Research *275*, 126-130. https://doi.org/10.1016/j.bbr.2014.09.008.
54. Lee, A.K., and Wilson, M.A. (2002). Memory of Sequential Experience in the Hippocampus during Slow Wave Sleep. Neuron *36*, 1183-1194. https://doi.org/10.1016/S0896-6273(02)01096-6.
55. Marshall, L., Helgadóttir, H., Mölle, M., and Born, J. (2006). Boosting slow oscillations during sleep potentiates memory. Nature *444*, 610-613. 10.1038/nature05278.
56. Rasch, B., Büchel, C., Gais, S., and Born, J. (2007). Odor Cues During Slow-Wave Sleep Prompt Declarative Memory Consolidation. Science *315*, 1426-1429. doi:10.1126/science.1138581.
57. Mander, B.A., Marks, S.M., Vogel, J.W., Rao, V., Lu, B., Saletin, J.M., Ancoli-Israel, S., Jagust, W.J., and Walker, M.P. (2015). β-amyloid disrupts human NREM slow waves and related hippocampus-dependent memory consolidation. Nature Neuroscience *18*, 1051-1057. 10.1038/nn.4035.
58. Jackson, C., McCabe, B.J., Nicol, A.U., Grout, A.S., Brown, M.W., and Horn, G. (2008). Dynamics of a Memory Trace: Effects of Sleep on Consolidation. Current Biology *18*, 393-400. https://doi.org/10.1016/j.cub.2008.01.062.
59. Gentner, T.Q., and Margoliash, D. (2003). Neuronal populations and single cells representing learned auditory objects. Nature *424*, 669-674. 10.1038/nature01731.
60. Carouso-Peck, S., and Goldstein, M.H. (2019). Female Social Feedback Reveals Non-imitative Mechanisms of Vocal Learning in Zebra Finches. Current Biology *29*, 631-636.e633. https://doi.org/10.1016/j.cub.2018.12.026.

61. Lipkind, D., and Tchernichovski, O. (2011). Quantification of developmental birdsong learning from the subsyllabic scale to cultural evolution. Proceedings of the National Academy of Sciences *108*, 15572-15579. doi:10.1073/pnas.1012941108.
62. Pravosudov, V.V., and Omanska, A. (2005). Dominance-related changes in spatial memory are associated with changes in hippocampal cell proliferation rates in mountain chickadees. Journal of Neurobiology *62*, 31-41. https://doi.org/10.1002/neu.20065.
63. Shettleworth, S.J., and Krebs, J.R. (1986). Stored and encountered seeds: A comparison of two spatial memory tasks in marsh tits and chickadees. Journal of Experimental Psychology: Animal Behavior Processes *12*, 248-257. 10.1037/0097-7403.12.3.248.
64. Funk, Chadd M., Honjoh, S., Rodriguez, Alexander V., Cirelli, C., and Tononi, G. (2016). Local Slow Waves in Superficial Layers of Primary Cortical Areas during REM Sleep. Current Biology *26*, 396-403. https://doi.org/10.1016/j.cub.2015.11.062.
65. Vyazovskiy, V.V., Olcese, U., Hanlon, E.C., Nir, Y., Cirelli, C., and Tononi, G. (2011). Local sleep in awake rats. Nature *472*, 443-447.
66. Rector, D.M., Topchiy, I.A., Carter, K.M., and Rojas, M.J. (2005). Local functional state differences between rat cortical columns. Brain research *1047*, 45-55.
67. Huber, R., Ghilardi, M.F., Massimini, M., Ferrarelli, F., Riedner, B.A., Peterson, M.J., and Tononi, G. (2006). Arm immobilization causes cortical plastic changes and locally decreases sleep slow wave activity. Nature neuroscience *9*, 1169-1176.
68. Riedner, B.A., Vyazovskiy, V.V., Huber, R., Massimini, M., Esser, S., Murphy, M., and Tononi, G. (2007). Sleep homeostasis and cortical synchronization: III. A high-density EEG study of sleep slow waves in humans. Sleep *30*, 1643-1657.
69. Letzner, S., Simon, A., and Güntürkün, O. (2016). Connectivity and neurochemistry of the commissura anterior of the pigeon (Columba livia). Journal of Comparative Neurology *524*, 343-361.
70. Paterson, A.K., and Bottjer, S.W. (2017). Cortical inter-hemispheric circuits for multimodal vocal learning in songbirds. Journal of Comparative Neurology *525*, 3312-3340.
71. Wyss, J.M., Swanson, L.W., and Cowan, W.M. (1980). The organization of the fimbria, dorsal fornix and ventral hippocampal commissure in the rat. Anatomy and Embryology *158*, 303-316. 10.1007/BF00301819.
72. Ball, N., Weaver, G., and Amlaner, C. (1986). The incidence of hemispheric sleep in birds. Sleep Res *15*, 58.
73. Ball, N., Amlaner, C., Shaffery, J., and Opp, M. (1988). Asynchronous eye-closure and unihemispheric quiet sleep of birds. Sleep *86*, 151-153.
74. Rattenborg, N.C., Lima, S.L., and Amlaner, C.J. (1999). Half-awake to the risk of predation. Nature *397*, 397-398. 10.1038/17037.
75. Rattenborg, N.C., Lima, S.L., and Amlaner, C.J. (1999). Facultative control of avian unihemispheric sleep under the risk of predation. Behavioural Brain Research *105*, 163-172.
76. Rattenborg, N., Amlaner, C., and Lima, S. (1999). Period amplitude analysis of avian unihemispheric quiet sleep. Sleep *22*, S73.
77. Rattenborg, N.C., Amlaner, C.J., and Lima, S.L. (2001). Unilateral eye closure and interhemispheric EEG asymmetry during sleep in the pigeon (Columba livia). Brain, behavior and evolution *58*, 323-332.
78. Szymczak, J., Kaiser, W., Helb, H., and Beszczyńska, B. (1996). A study of sleep in the European blackbird. Physiology & behavior *60*, 1115-1120.
79. Wellmann, A.E., and Downs, C.T. (2009). A behavioural study of sleep patterns in the malachite sunbird, Cape white-eye and fan-tailed widowbird. Animal Behaviour *77*, 61-66.
80. Ridgway, S.H. (1986). Physiological observations on dolphin brains. Dolphin cognition and behavior: A comparative approach, 31-59.
81. Tarpley, R.J., and Ridgway, S.H. (1994). Corpus callosum size in delphinid cetaceans. Brain, Behavior and Evolution *44*, 156-165.

82. Wallman, J., and Pettigrew, J.D. (1985). Conjugate and disjunctive saccades in two avian species with contrasting oculomotor strategies. Journal of Neuroscience *5*, 1418-1428.
83. Schaeffel, F., Howland, H.C., and Farkas, L. (1986). Natural accommodation in the growing chicken. Vision Research *26*, 1977-1993.
84. Assaf, Y., Bouznach, A., Zomet, O., Marom, A., and Yovel, Y. (2020). Conservation of brain connectivity and wiring across the mammalian class. Nature Neuroscience *23*, 805-808. 10.1038/s41593-020-0641-7.
85. Krupnik, R., Yovel, Y., and Assaf, Y. (2021). Inner Hemispheric and Interhemispheric Connectivity Balance in the Human Brain. The Journal of Neuroscience *41*, 8351-8361. 10.1523/jneurosci.1074-21.2021.
86. Lee, J.M., Kyeong, S., Kim, E., and Cheon, K.-A. (2016). Abnormalities of Inter- and Intra-Hemispheric Functional Connectivity in Autism Spectrum Disorders: A Study Using the Autism Brain Imaging Data Exchange Database. Frontiers in Neuroscience *10*. 10.3389/fnins.2016.00191.
87. Yao, S., Becker, B., and Kendrick, K.M. (2021). Reduced Inter-hemispheric Resting State Functional Connectivity and Its Association With Social Deficits in Autism. Frontiers in Psychiatry *12*. 10.3389/fpsyt.2021.629870.
88. Chang, X., Collin, G., Mandl, R.C.W., Cahn, W., and Kahn, R.S. (2019). Interhemispheric connectivity and hemispheric specialization in schizophrenia patients and their unaffected siblings. NeuroImage: Clinical *21*, 101656. https://doi.org/10.1016/j.nicl.2019.101656.
89. Zhu, F., Liu, F., Guo, W., Chen, J., Su, Q., Zhang, Z., Li, H., Fan, X., and Zhao, J. (2018). Disrupted asymmetry of inter- and intra-hemispheric functional connectivity in patients with drug-naive, first-episode schizophrenia and their unaffected siblings. eBioMedicine *36*, 429-435. 10.1016/j.ebiom.2018.09.012.
90. Vink, J., Westover, M., Pascual-Leone, A., and Shafi, M. (2019). EEG functional connectivity predicts causal brain interactions. Brain Stimulation: Basic, Translational, and Clinical Research in Neuromodulation *12*, 449. 10.1016/j.brs.2018.12.458.
91. Massimini, M., Ferrarelli, F., Huber, R., Esser, S.K., Singh, H., and Tononi, G. (2005). Breakdown of cortical effective connectivity during sleep. Science *309*, 2228-2232.
92. Douw, L., de Groot, M., van Dellen, E., Heimans, J.J., Ronner, H.E., Stam, C.J., and Reijneveld, J.C. (2010). 'Functional Connectivity' Is a Sensitive Predictor of Epilepsy Diagnosis after the First Seizure. PLOS ONE *5*, e10839. 10.1371/journal.pone.0010839.
93. Behroozi, M., Helluy, X., Ströckens, F., Gao, M., Pusch, R., Tabrik, S., Tegenthoff, M., Otto, T., Axmacher, N., Kumsta, R., et al. (2020). Event-related functional MRI of awake behaving pigeons at 7T. Nature Communications *11*, 4715. 10.1038/s41467-020-18437-1.
94. De Groof, G., and Van der Linden, A. (2010). Love songs, bird brains and diffusion tensor imaging. NMR in biomedicine *23*, 873-883.
95. De Groof, G., Verhoye, M., Van Meir, V., Tindemans, I., Leemans, A., and Van der Linden, A. (2006). In vivo diffusion tensor imaging (DTI) of brain subdivisions and vocal pathways in songbirds. Neuroimage *29*, 754-763.
96. De Groof, G., Verhoye, M., Van Meir, V., Balthazart, J., and Van der Linden, A. (2008). Seasonal rewiring of the songbird brain: an in vivo MRI study. European Journal of Neuroscience *28*, 2475-2485.
97. Corballis, M.C. (2009). The evolution and genetics of cerebral asymmetry. Philosophical Transactions of the Royal Society B: Biological Sciences. Royal Society.
98. Corballis, M.C. (2010). Handedness and cerebral asymmetry: An evolutionary perspective.
99. Corballis, M.C. (2019). Evolution of cerebral asymmetry. Progress in Brain Research *250*, 153-178.
100. Schaafsma, S., Riedstra, B., Pfannkuche, K., Bouma, A., and Groothuis, T. (2009). Epigenesis of behavioural lateralization in humans and other animals. Philosophical Transactions of the Royal Society B: Biological Sciences *364*, 915-927.
101. Rogers, L.J. (2009). Hand and paw preferences in relation to the lateralized brain. Philosophical Transactions of the Royal Society B: Biological Sciences *364*, 943-954.

102. Forrester, G., Hudry, K., Lindell, A., and Hopkins, W.D. (2018). Cerebral lateralization and cognition: evolutionary and developmental investigations of behavioral biases (Academic Press).
103. Emerson, R.W., Gao, W., and Lin, W. (2016). Longitudinal Study of the Emerging Functional Connectivity Asymmetry of Primary Language Regions during Infancy. The Journal of Neuroscience *36*, 10883-10892. 10.1523/jneurosci.3980-15.2016.
104. Raemaekers, M., Schellekens, W., Petridou, N., and Ramsey, N.F. (2018). Knowing left from right: asymmetric functional connectivity during resting state. Brain Structure and Function *223*, 1909-1922. 10.1007/s00429-017-1604-y.
105. Chirathivat, N., Raja, S.C., and Gobes, S.M.H. (2015). Hemispheric dominance underlying the neural substrate for learned vocalizations develops with experience. Scientific Reports *5*, 11359. 10.1038/srep11359.
106. Moorman, S., Gobes, S.M., Kuijpers, M., Kerkhofs, A., Zandbergen, M.A., and Bolhuis, J.J. (2012). Human-like brain hemispheric dominance in birdsong learning. Proceedings of the National Academy of Sciences *109*, 12782-12787.
107. Sanders, J.I., and Kepecs, A. (2014). A low-cost programmable pulse generator for physiology and behavior. Frontiers in Neuroengineering *7*. 10.3389/fneng.2014.00043.
108. Siegle, J.H., López, A.C., Patel, Y.A., Abramov, K., Ohayon, S., and Voigts, J. (2017). Open Ephys: An open-source, plugin-based platform for multichannel electrophysiology. Journal of Neural Engineering *14*. 10.1088/1741-2552/aa5eea.
109. Wildman, J. (2022). Bron-Kerbosch maximal clique finding algorithm https://www.mathworks.com/matlabcentral/fileexchange/30413-bron-kerbosch-maximal-clique-finding-algorithm.